Research Article

URF PUBLISHERS
connect with research world

Journal of Petroleum & Chemical Engineering

https://urfpublishers.com/journal/petrochemical-engineering

Vol: 3 & Iss: 2

Analysis and Control of Alzheimer's Disease Models

Lakshmi N Sridhar*

Chemical Engineering Department, University of Puerto Rico, Mayaguez, PR 00681-9046, USA

Citation: Sridhar LN. Analysis and Control of Alzheimer's Disease Models. *J Petro Chem Eng* 2025;3(2):111-118.

Received: 23 May, 2025; **Accepted:** 26 June, 2025; **Published:** 28 June, 2025

***Corresponding author:** Lakshmi N Sridhar, Chemical Engineering Department, University of Puerto Rico, Mayaguez, PR 00681, USA, E-mail: lakshmin.sridhar@upr.edu

ABSTRACT

Millions of people are affected by Alzheimer's disease, which is a progressive neurodegenerative disorder. It is important to understand the progression dynamics of this disease to be able to minimize the damage that is caused by it. This article provides a mathematical framework to develop strategies to slow down the progression of Alzheimer's disease. Bifurcation analysis is a powerful mathematical tool used to deal with the nonlinear dynamics of any process. Several factors must be considered and multiple objectives must be met simultaneously. Bifurcation analysis and multiobjective nonlinear model predictive control (MNLMPC) calculations are performed on two Alzheimer's disease models. The MATLAB program MATCONT was used to perform the bifurcation analysis. The MNLMPC calculations were performed using the optimization language PYOMO in conjunction with the state-of-the-art global optimization solvers IPOPT and BARON. The bifurcation analysis revealed the existence of limit points in the models. The limit points were beneficial because they enabled the multiobjective nonlinear model predictive control calculations to converge to the Utopia point in both problems, which is the most beneficial solution. A combination of bifurcation analysis and multiobjective nonlinear model predictive control for Alzheimer's disease models is the main contribution of this paper.

Keywords: Alzheimer's disease; Bifurcation; Optimization; Control

Background

Chao, et al[1], discussed the transforming growth factor beta in Alzheimer's disease. Lue, et al[2], showed that the soluble amyloid beta peptide concentration is a predictor of synaptic change in Alzheimer's disease. Mehta, et al[3], investigated the plasma and cerebrospinal fluid levels of amyloid β proteins 1-40 and 1-42 in Alzheimer disease. Penkowa, et al[4], showed the impaired inflammatory response and increased oxidative stress and neurodegeneration after brain injury in interleukin-6-deficient mice. Penkowa, et al[5], demonstrated that the Interleukin-6 deficiency reduces the brain inflammatory response and increases oxidative stress and neurodegeneration after kainic acid-induced seizures. Wyss-Coray, et al[6], showed that TGF-β1 promotes microglial amyloid-β clearance and reduces plaque burden in transgenic mice. Jacobsen, et al[7], investigated the early-onset behavioral and synaptic deficits in a mouse model of Alzheimer's disease. Wyss-Coray[8] showed that the TGF-β pathway was a potential target in neurodegeneration and Alzheimer's disease. Das, et al[9], demonstrated the dysfunction of TGF-β signaling in Alzheimers disease. Tobinick, et al[10], used the TNF-alpha modulation for treatment of Alzheimer's disease. Green, et al[11], investigated the role of calcium in the pathogenesis of Alzheimer's disease and transgenic models. Group, et al[12], showed that naproxen and celecoxib do not prevent AD in early results from a randomized controlled trial. Town, et al[13], demonstrated that. blocking TGF-β–smad2/3 innate immune signaling mitigates Alzheimer-like pathology. Cheung, et al[14], illustrated the mechanism of Ca2+ disruption in

Alzheimer's disease by presenilin regulation of InsP3 receptor channel gating. Bezprozvanny, et al[15], researched the neuronal calcium mishandling and the pathogenesis of Alzheimer's disease. Bojarski, et al[16], investigated the calcium dysregulation in Alzheimer's disease. Group, et al[17], researched the cognitive function over time in the Alzheimer's Disease and produced results of a randomized, controlled trial of naproxen and celecoxib.

Lopez, et al[18], J., Lyckman, A., Oddo, S., LaFerla, F., Querfurth, H., Shtifman, A., 2008. Increased intraneuronal resting [Ca2+] in adult Alzheimer's disease mice. Nelson, et al[19], investigated familial Alzheimer's disease mutations in presenilins and studied the effects on endoplasmic reticulum calcium homeostasis and correlation with clinical phenotypes. Puri, et al[20], studied Mathematical models for the pathogenesis of Alzheimer's disease. Berridge[21], tested the calcium hypothesis of Alzheimer's disease. Eur. J. Physiol. 459, 441-449. Imbimbo, et al[22], investigated whether NSAIDs are useful to treat Alzheimer's disease or mild cognitive impairment. Berridge[23], studied the effect of calcium signalling on Alzheimer's disease. Anastasio[24], performed data-driven modelling of Alzheimer's disease pathogenesis. Camandola and Mattson[25], studied the aberrant subcellular neuronal calcium regulation in aging and Alzheimer's disease. Ho, et al[26], showed that the effects of metal chelators on γ-secretase indicate that calcium and magnesium ions facilitate cleavage of Alzheimer's amyloid precursor substrate. Itkin, et al[27], demonstrated that calcium ions promote the formation of amyloid b-peptide (1-40) oligomers causally implicated in neuronal toxicity of Alzheimer's disease. Müller, et al[28], studied the constitutive cAMP response element binding protein (CREB) activation by Alzheimer's disease presenilin-driven inositol trisphosphate receptor (InsP3R) Ca2+ signaling.

Schmidt, et al[29], performed quantitative modelling of amyloidogenic processing and its influence by SORLA in Alzheimer's disease. Ma, et al[30], studied mitochondrial modulation of store-operated Ca2+ entry in model cells of Alzheimer's disease. Woods and Padmanabhan[31], studied the effect of neuronal calcium signaling on Alzheimer's disease. De Kimpe, et al[32], showed that disturbed Ca2+ homeostasis increases glutaminyl cyclase expression, connecting two early pathogenic events in Alzheimer's disease in vitro. Berridge, M[33], investigated the dysregulation of neural calcium signaling in Alzheimer's disease. Cabezas, et al[34], investigated the role of glial cells in Alzheimer's disease. Chen, et al[35], studied strategies involving protection of TGF-β1 against neuroinflammation and neurodegeneration in Aβ1-42-induced Alzheimer's disease in model rats. Von Bernhardi, et al[36], studied the role of TGFβ signaling in the pathogenesis of Alzheimer's disease. Bertsch, et al[37] and Hao, et al[38] developed mathematical models for the onset and progression of Alzheimer's disease. Forloni, et al[39], performed research involving oligomers and inflammation in Alzheimer's disease.

Kinney, et al[40], conclude that inflammation is a central mechanism in Alzheimer's disease. Zhu, et al[41], investigated whether inflammation be resolved in Alzheimer's disease. Ozben, et al[42], studied neuro-inflammation and anti-inflammatory treatment options for Alzheimer's disease. Ali, et al[43], provide recommendations for anti-inflammatory treatments in Alzheimer's disease. Ciuperca, et al[44], developed an in vitro mathematical model involving Alzheimer's disease and prions. Andrade-Restrepo, et al[45], modelled the spatial propagation of Aβ oligomers in Alzheimer's disease. Rivers-Auty, et al[46], investigated the use of anti-inflammatories in Alzheimer's disease-potential therapy. Huang, et al[47], performed clinical trials of new drugs for Alzheimer's disease. Li, et al[48], developed a mathematical model of Alzheimer's disease with prion proteins interactions and treatment. Hu, et al[49], performed optimal control calculations of a stochastic reaction diffusion model for Alzheimer's disease with impulse and time-varying delay. Hao, et al[50], developed a strategy for optimal anti-amyloid-beta therapy for Alzheimer's disease via a personalized mathematical model. Al-Ghraiybah, et al[51], studied glial cell-mediated neuroinflammation in Alzheimer's disease. Pal et al[52], modelled Anti-Amyloid-Beta Therapy for Alzheimer's Disease. Van Dyck et al[53], investigated Lecanemab in early Alzheimer's disease. Ciuperca, et al[54], performed a qualitative analysis of an A β-monomer model with inflammation processes for Alzheimer's disease. Caluwé, et al[55], discuss he progression towards Alzheimer's disease described as a bistable switch arising from the positive loop between amyloids and Ca2+.

Torres, et al[56], performed optimal control calculations involving anti-inflammatory treatments of Alzheimer's disease. All the optimal control work involving Alzheimer's disease involved single-objective optimal control. In this article we perform multiobjective nonlinear model predictive control in conjunction with bifurcation analysis for two Alzheimer's disease. The two models that will be used are the ones described in Caluwé, et al[55] and Ciuperca et al[54]. These models will be referred to as model 1 and model 2. This paper is organized as follows. First, the Alzheimer's disease models are presented. The numerical procedures (bifurcation analysis and multiobjective nonlinear model predictive control (MNLMPC) are then described. This is followed by the results and discussion and conclusions.

Alzheimer's Disease Models

Model 1

The model equations are

$$\frac{da}{dt} = v_1 - k_1 a + \frac{v_\alpha (c^n)}{((k_\alpha{}^n) + (c^n))};$$

$$\frac{dc}{dt} = v2 - (k_2 c) + k_\beta (a^m);$$

The parameter values are

$$v_\alpha = 0.05;\ k_\alpha = 120; n = 2; k_1 = 0.01; k_\beta = 0.2; m = 4; k_2 = 0.1;$$

a and c represent the concentrations of Aβ and the intracellular Ca2+. v_1, v_2 represent the synthesis rate of Aβ and the rate at which Ca2+ enters the cytoplasm. These are the bifurcation and control parameters, respectively.

Model 2

The model equations are

$$\frac{db}{dt} = r_1 (mval)^2 - \gamma_0 (b)$$

$$\frac{db_p}{dt} = \gamma_0 (b) - \tau_p b_p$$

$$\frac{d(mval)}{dt} = \frac{\tau_S (ival)}{(1 + (c(b^{mval}))} - d(mval) - r_2 (b) mval - r_1 (mval)^2$$

$$\frac{d(mcap)}{dt} = \frac{\alpha_1 b(mcap)(\hat{m} - mcap)}{(1+(\alpha_2 b))} - sigma(mcap) - \lambda_M$$

$$\frac{d(ival)}{dt} = \frac{\tau_1 b(mcap)}{(1+(\tau_2 b))} - \tau_3(ival)$$

The parameter values are

$$r_1 = 0.1; r_2 = 0.1; \gamma_0 = 0.0\,5;\ \tau_1 = 1; \tau_2 = 1; \tau_3 = 1;$$

$$\tau_p = 0.03; \tau_s = 1;\ c = 1; nval = 2; \alpha_1 = 1; \alpha_2 = 1; \lambda_M = 1.e-03;\ \hat{m} = 1;$$

b and bp represent the oligomer concentration and the concentration of oligomers in plaques. mval and mcap represent the monomer and microglial cell concentrations. ival represents the interleukin concentration. Sigma and d are the degradation rates of microglial cells and the degradation rate of monomers. These are the bifurcation and control parameters, respectively.

Bifurcation Analysis

The MATLAB software MATCONT is used to perform the bifurcation calculations. Bifurcation analysis deals with multiple steady-states and limit cycles. Multiple steady states occur because of the existence of branch and limit points. Hopf bifurcation points cause limit cycles. A commonly used MATLAB program that locates limit points, branch points and Hopf bifurcation points is MATCONT[57,58]. This program detects Limit points (LP), branch points (BP) and Hopf bifurcation points(H) for an ODE system.

$$\frac{dx}{dt} = f(x, \alpha)$$

$x \in R^n$ Let the bifurcation parameter be α Since the gradient is orthogonal to the tangent vector,

The tangent plane at any point $w = [w_1, w_2, w_3, w_4, ...w_{n+1}]$ must satisfy

$$Aw = 0$$

Where A is

$$A = [\partial f / \partial x \quad | \partial f / \partial \alpha]$$

where $\partial f / \partial x$ is the Jacobian matrix. For both limit and branch points, the matrix $[\partial f / \partial x]$ must be singular. The n+1 th component of the tangent vector $w_{n+1} = 0$ for a limit point (LP)and for a branch point (BP) the matrix $\begin{bmatrix} A \\ w^T \end{bmatrix}$ must be singular. At a Hopf bifurcation point,

$$\det(2 f_x(x, \alpha) @ I_n) = 0$$

@ indicates the BI alternate product while is the n-square identity matrix. Hopf bifurcations cause limit cycles and should be eliminated because limit cycles make optimization and control tasks very difficult. More details can be found in Kuznetsov and Govaerts[59-61].

Nonlinear Model Predictive Control (MNLMPC)

Flores Tlacuahuaz, et al[62], developed a multiobjective nonlinear model predictive control (MNLMPC) method that is rigorous and does not involve weighting functions or additional constraints. This procedure is used for performing the MNLMPC calculations Here $\sum_{t_i=0}^{t_i=t_f} q_j(t_i)$ (j=1, 2..n) represents the variables that need to be minimized/maximized simultaneously for a problem involving a set of ODE

$$\frac{dx}{dt} = F(x, u)$$

t_f being the final time value and n the total number of objective variables and. u the control parameter. This MNLMPC procedure first solves the single objective optimal control problem independently optimizing each of the variables $\sum_{t_i=0}^{t_i=t_f} q_j(t_i)$ individually. The minimization/maximization of $\sum_{t_i=0}^{t_i=t_f} q_j(t_i)$ will lead to the values q_j^* . Then the optimization problem that will be solved is

$$\min\left(\sum_{j=1}^{n}\left(\sum_{t_i=0}^{t_i=t_f} q_j(t_i) - q_j^*\right)\right)^2$$

$$subject\ to\ \frac{dx}{dt} = F(x, u);$$

This will provide the values of u at various times. The first obtained control value of u is implemented and the rest are discarded. This procedure is repeated until the implemented and the first obtained control values are the same or if the Utopia point where ($\sum_{t_i=0}^{t_i=t_f} q_j(t_i) = q_j^*$ for all j) is obtained.

Pyomo[63], is used for these calculations. Here, the differential equations are converted to a Nonlinear Program (NLP) using the orthogonal collocation method The NLP is solved using IPOPT[64] and confirmed as a global solution with BARON[65].

The steps of the algorithm are as follows

- Optimize $\sum_{t_i=0}^{t_i=t_f} q_j(t_i)$ and obtain q_j^* at various time intervals t_i. The subscript *i* is the index for each time step.
- Minimize $\left(\sum_{j=1}^{n}\left(\sum_{t_i=0}^{t_i=t_f} q_j(t_i) - q_j^*\right)\right)^2$ and get the control values for various times.
- Implement the first obtained control values
- Repeat steps 1 to 3 until there is an insignificant difference between the implemented and the first obtained value of the control variables or if the Utopia point is achieved. The Utopia point is when $\sum_{t_i=0}^{t_i=t_f} q_j(t_i) = q_j^*$ for all j.

Sridhar[66], proved that the MNLMPC calculations to converge to the Utopia solution when the bifurcation analysis revealed the

presence of limit and branch points. This was done by imposing the singularity condition on the co-state equation[67]. If the minimization of q_1 lead to the value q_1^* and the minimization of q_2 lead to the value q_2^* The MNLPMC calculations will minimize the function $(q_1-q_1^*)^2+(q_2-q_2^*)^2$. The multiobjective optimal control problem is

$$\min \quad (q_1-q_1^*)^2+(q_2-q_2^*)^2 \quad subject\ to \quad \frac{dx}{dt}=F(x,u)$$

Differentiating the objective function results in

$$\frac{d}{dx_i}((q_1-q_1^*)^2+(q_2-q_2^*)^2)=2(q_1-q_1^*)\frac{d}{dx_i}(q_1-q_1^*)+2(q_2-q_2^*)\frac{d}{dx_i}(q_2-q_2^*)$$

The Utopia point requires that both $(q_1-q_1^*)$ and $(q_2-q_2^*)$ are zero. Hence

$$\frac{d}{dx_i}((q_1-q_1^*)^2+(q_2-q_2^*)^2)=0$$

the optimal control co-state equation is

$$\frac{d}{dt}(\lambda_i)=-\frac{d}{dx_i}((q_1-q_1^*)^2+(q_2-q_2^*)^2)-f_x\lambda_i;\quad \lambda_i(t_f)=0$$

λ_i is the Lagrangian multiplier. t_f is the final time. The first term in this equation is 0 and hence

$$\frac{d}{dt}(\lambda_i)=-f_x\lambda_i;\lambda_i(t_f)=0$$

At a limit or a branch point, for the set of ODE $\frac{dx}{dt}=f(x,u)$ f_x is singular. Hence there are two different vectors-values for $[\lambda_i]$ where $\frac{d}{dt}(\lambda_i)>0$ and $\frac{d}{dt}(\lambda_i)<0$. In between there is a vector $[\lambda_i]$ where $\frac{d}{dt}(\lambda_i)=0$. This coupled with the boundary condition $\lambda_i(t_f)=0$ will lead to $[\lambda_i]=0$ This makes the problem an unconstrained optimization problem and the only solution is the Utopia solution.

Results and Discussion

Bifurcation analysis for model 1 revealed the existence of limit points for both the bifurcation parameters v1 and v2. The coordinates for the 2 limit points are (a,c,v1) = (1.682845, 56.040073, 0.007876) and (a,c,v2) = (1.672121, 60.828416, 4.519333). These limit points are shown in **(Figures 1a and 1b)**.

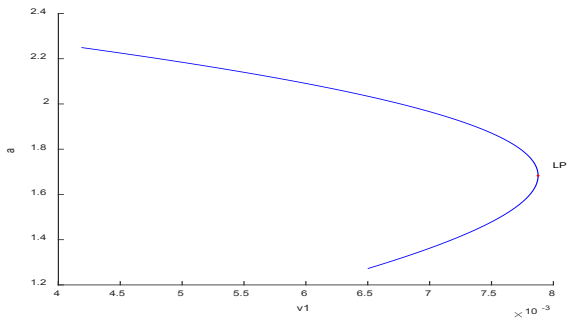

Figure 1a: Biurcation analysis model 1 v1 is bifurcation parameter.

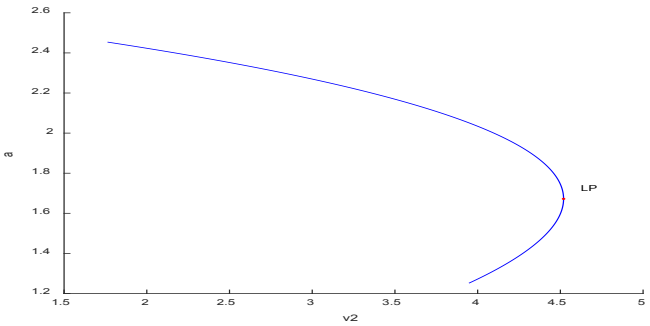

Figure 1b: Biurcation analysis model 1 v2 is bifurcation parameter.

The variables, a and c, which are the concentrations of Aβ and the intracellular Ca2+were minimized. $\sum_{t_i=0}^{t_i=t_f} a(t_i)$, $\sum_{t_i=0}^{t_i=t_f} b(t_i)$, was minimized individually and each of them led to a value of 0. The overall optimal control problem will involve the minimization of $(\sum_{t_i=0}^{t_i=t_f} a(t_i)-0)^2+(\sum_{t_i=0}^{t_i=t_f} b(t_i)-0)^2$ was minimized subject to the equations governing the model. This led to a value of zero (the Utopia solution.

The various concentration profiles for this MNLMPC calculation are shown in **(Figures 1c-1d)**.

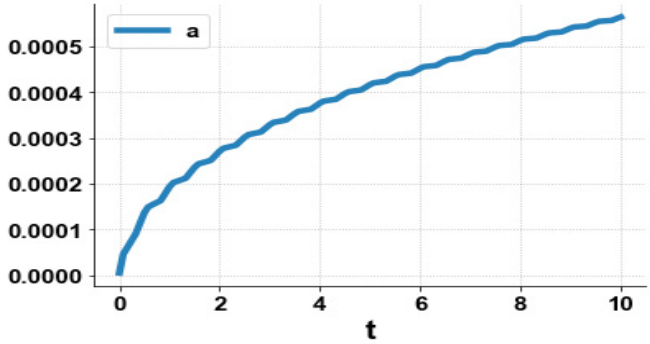

Figure 1c: MNLMPC model a vs t.

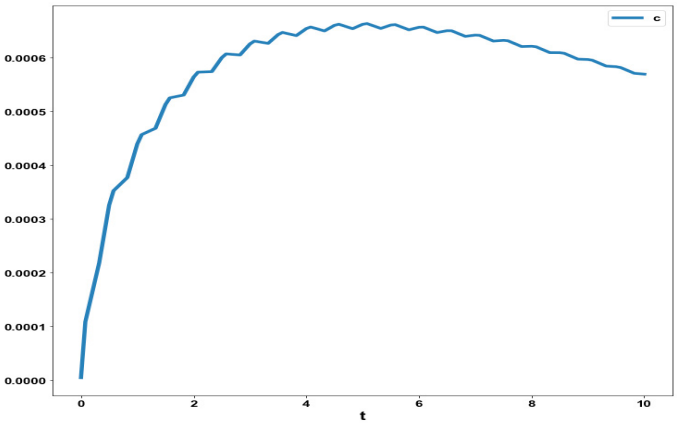

Figure 1d: MNLMPC model 1 c vs t.

The obtained control profile of s exhibited noise **(Figures 1e-1h)**. This was remedied using the Savitzky-Golay Filter. The smoothed-out version of this profile is shown in Figs 1g and 1h. The MNLMPC control values obtained for v1 and v2 are 0.00039 v2 0.001017.

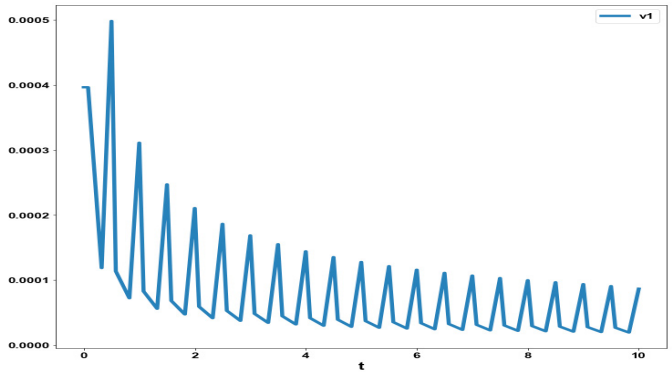

Figure 1e: MNLMPC model 1 v1 vs t.

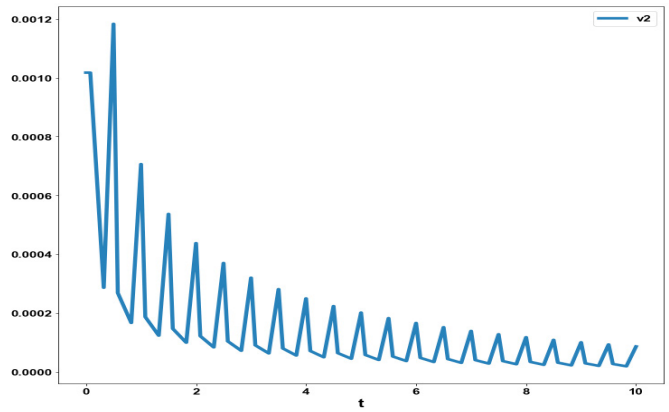

Figure 1f: MNLMPC model 1 v2 vs t.

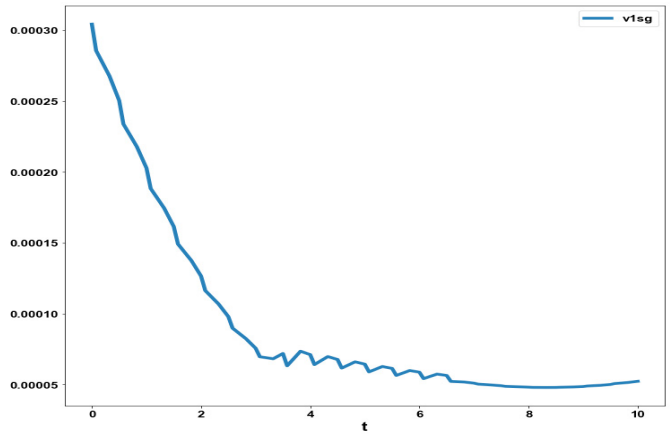

Figure 1g: MNLMPC model 1 v1 (Savitzky Golay) vs t.

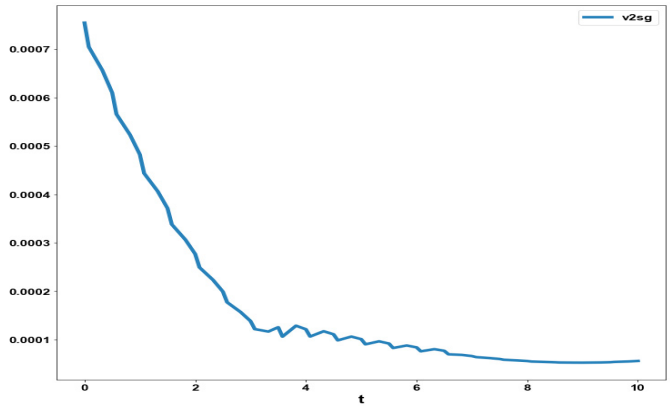

Figure 1h: MNLMPC model 1 v2 (Savitzky Golay) vs t.

Bifurcation analysis for model 2 revealed the existence of limit points for both the bifurcation parameters sigma and d.

The coordinates for the 2 limit points are (b, bp, mval, mcap, ival, sigma) = (0.557430, 0.929049, 0.527934, 0.499842, 0.178902, 0.177014) and (b, bp, mval, mcap, ival, d) = (0.310730, 0.517884, 0.394164, 0.991528, 0.235058, 0.473347). These limit points are shown in **(Figures 2a and 2b)**. The variables b and bp which are the oligomer concentration and the concentration of oligomers in plaques were minimized. $\sum_{i=0}^{t_i=t_f} b(t_i), \sum_{i=0}^{t_i=t_f} bp(t_i)$, was minimized individually and each of them led to a value of 0. The overall optimal control problem will involve the minimization of $(\sum_{i=0}^{t_i=t_f} b(t_i)-0)^2+(\sum_{i=0}^{t_i=t_f} bp(t_i)-0)^2$ was minimized subject to the equations governing the model. This led to a value of zero (the Utopia solution. The various concentration profiles for this MNLMPC calculation are shown in **(Figures 2c-2g)**. The obtained control profile of s exhibited noise **(Figures 2h and 2i)**. This was remedied using the Savitzky-Golay Filter. The smoothed-out version of this profile is shown in **(Figures 2j and 2k)**. The MNLMPC control values obtained for sigma and d are 0.2499 and 0.5683.

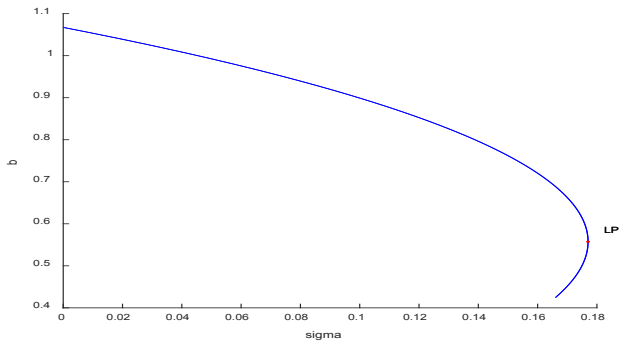

Figure 2a: (Bifurcation diagram model 2 sigma is bifurcation parameter).

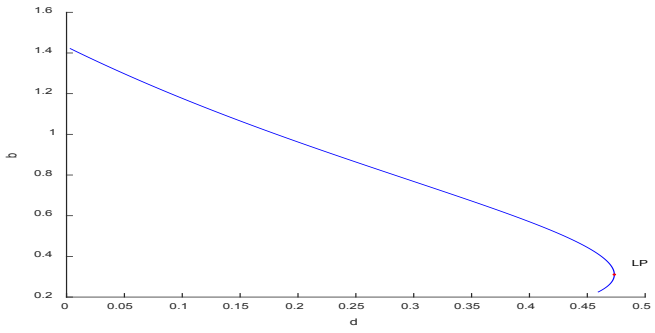

Figure 2b: (Bifurcation diagram model 2 d is bifurcation parameter).

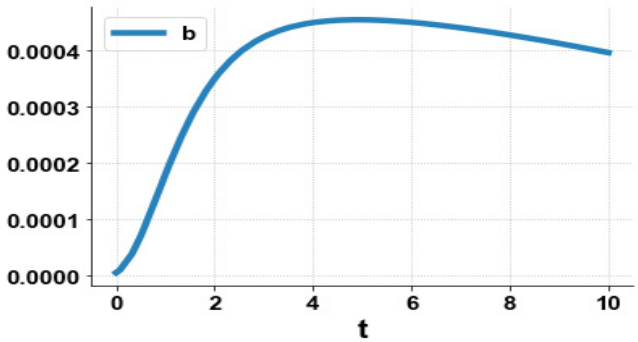

Figure 2c: MNLMPC model 2 b vs t.

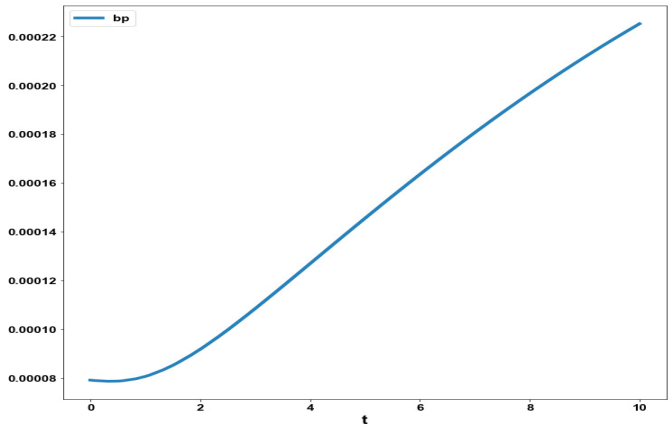

Figure 2d: MNLMPC model 2 bp vs t

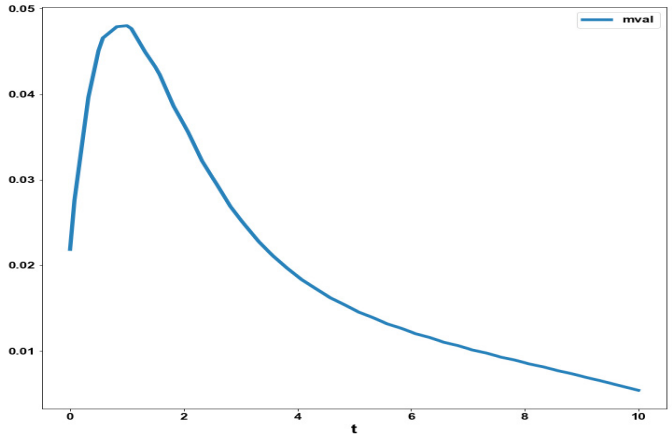

Figure 2e: MNLMPC model mval vs t.

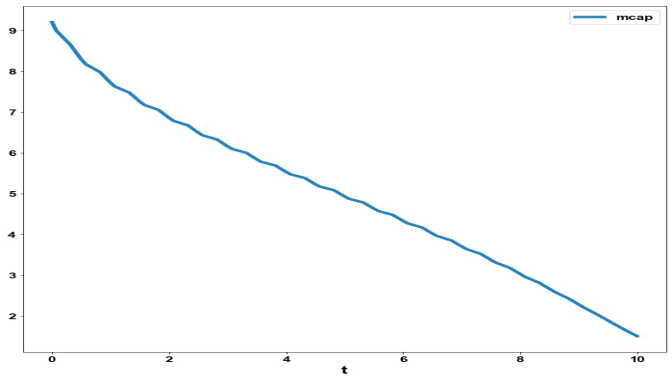

Figure 2f: MNLMPC model mcap vs t

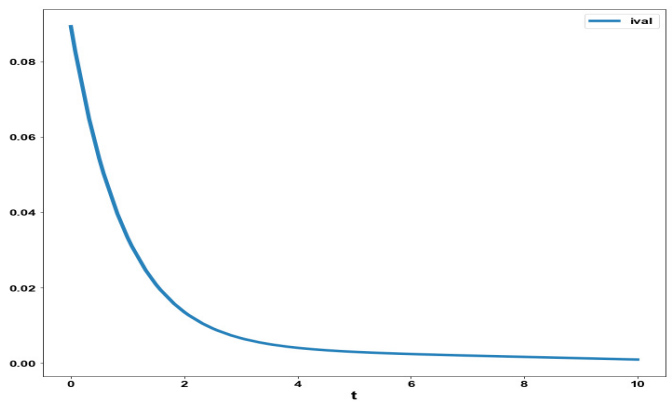

Figure 2g: MNLMPC model ival vs t.

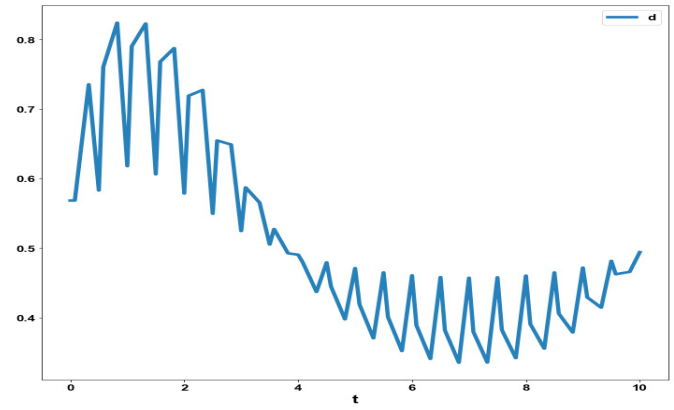

Figure 2h: MNLMPC model d vs t.

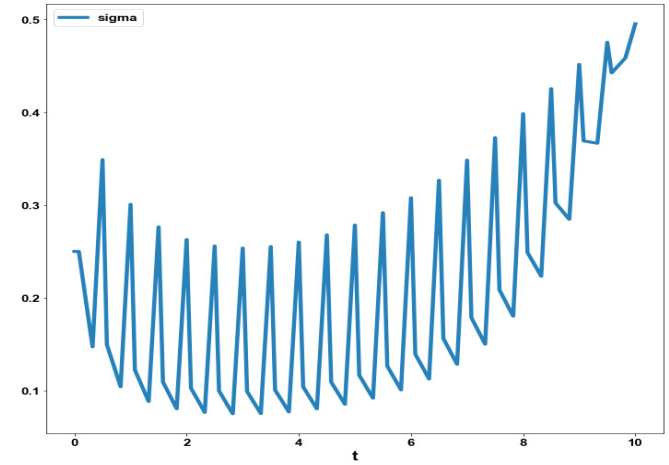

Figure 2i: (MNLMPC model 2 sigma vs t).

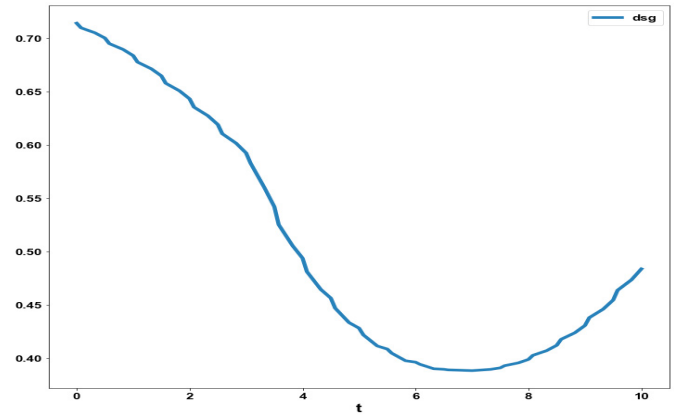

Figure 2j: (MNLMPC d (Savitzky Golay) vs t).

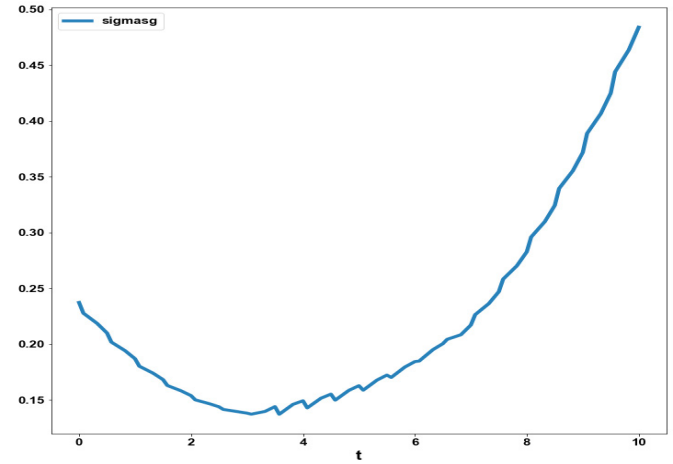

Figure 2k: MNLMPC model 2 sigma (Savitzky Golay) vs t.

In both the cases, the MNLMPC calculations converged to the Utopia solution, validating the analysis of Sridhar[66], which showed that the presence of a limit point enables the MNLMPC calculations to reach the best possible (Utopia) solution.

Conclusion

Bifurcation analysis and Multiobjective nonlinear model predictive control calculations were performed on two Alzheimer's disease models. The bifurcation analysis revealed the existence of linit points. The limit points (which produced multiple steady-state solutions originating from a singular point) are very beneficial as they caused the multiojective nonlinear model predictive calculations to converge to the Utopia point (the best possible solution) in both models. A combination of bifurcation analysis and multiobjective nonlinear model predictive control for Alzheimer's disease models is the main contribution of this paper.

Data Availability Statement

All data used is presented in the paper.

Conflict of Interest

The author, Dr. Lakshmi N Sridhar has no conflict of interest.

Acknowledgement

Dr. Sridhar thanks Dr. Carlos Ramirez and Dr. Suleiman for encouraging him to write single-author papers.

References

1. Chao C, Hu S, Frey 2nd W, Ala T, Tourtellotte W, Peterson P. Transforming growth factor beta in Alzheimer's disease. Clin Diagnostic Laboratory Immunology 1994;1(1):109-110.
2. Lue L, Kuo Y, Roher A, et al. Soluble amyloid beta peptide concentration as a predictor of synaptic change in Alzheimer's disease. Am J Pathol 1999;155:853-862.
3. Mehta PD, Pirttila T, Mehta SP, Sersen EA, Aisen PS, Wisniewski HM. Plasma and cerebrospinal fluid levels of amyloid β proteins 1-40 and 1-42 in Alzheimer disease. Archives of neurology 2000;57(1):100-105.
4. Penkowa M, Giralt M, Carrasco J, Hadberg H, Hidalgo J. Impaired inflammatory response and increased oxidative stress and neurodegeneration after brain injury in interleukin-6-deficient mice. Glia 2000;32(3):271-285.
5. Penkowa M, Molinero A, Carrasco J, Hidalgo J. Interleukin-6 deficiency reduces the brain inflammatory response and increases oxidative stress and neurodegeneration after kainic acid-induced seizures. Neuroscience 2001;102(4):805-818.
6. Wyss-Coray T, Lin C, Yan F, et al. TGF-β1 promotes microglial amyloid-β clearance and reduces plaque burden in transgenic mice. Nature med 2001;7(5):612-618.
7. Jacobsen J, Wu C, Redwine J, et al. Early-onset behavioral and synaptic deficits in a mouse model of Alzheimer's disease. Proc Natl Acad Sci USA 2006;103:5161-5166.
8. Wyss-Coray T. TGF-β pathway as a potential target in neurodegeneration and Alzheimer's. Current Alzheimer Res 2006;3(3):191-195.
9. Das P, Golde T, et al. Dysfunction of TGF-β signaling in Alzheimer's disease. J clin investigation 2006;116(11):2855-2857.
10. Tobinick E, Gross H, Weinberger A, Cohen H. TNF-alpha modulation for treatment of Alzheimer's disease: a 6-month pilot study. Medscape General Med 2006;8(2):25.
11. Green KN, Smith I, LaFerla F. Role of calcium in the pathogenesis of Alzheimer's disease and transgenic models. Subcell Biochem 2007;45:507-521.
12. Group AR, Lyketsos CG, Breitner JCS, et al. Naproxen and celecoxib do not prevent AD in early results from a randomized controlled trial. Neurology 2007;68(21):1800-1808.
13. Town T, Laouar Y, Pittenger C, et al. Blocking TGF-β–Smad2/3 innate immune signaling mitigates Alzheimer-like pathology. Nature medicine 2008;14(6):681-687.
14. Cheung K-H, Shineman D, Muller M, et al. Mechanism of Ca2+ disruption in Alzheimer's disease by presenilin regulation of InsP3 receptor channel gating. Neuron 2008;56:871-883.
15. Bezprozvanny I, Mattson MP. Neuronal calcium mishandling and the pathogenesis of Alzheimer's disease. Trends Neurosci 2008;31:454-463.
16. Bojarski L, Herms J, Kuznicki J. Calcium dysregulation in Alzheimer's disease. Neurochem. Int 2008;52:621-633.
17. Group AR, Martin BK, Szekely C, et al. Cognitive function over time in the Alzheimer's Disease Anti-inflammatory Prevention Trial (ADAPT): results of a randomized, controlled trial of naproxen and celecoxib. Archives of neurology 2008;65(7):896.
18. Lopez J, Lyckman A, Oddo S, LaFerla F, Querfurth H, Shtifman A. Increased intraneuronal resting [Ca2+] in adult Alzheimer's disease mice. J. Neurochem 2008;105:262-271.
19. Nelson O, Supnet C, Liu H, Bezprozvanny I. Familial Alzheimer's disease mutations in presenilins. Effects on endoplasmic reticulum calcium homoeostasis and correlation with clinical phenotypes. J Alzheimer's Dis 2010;21:781-793.
20. Puri IK, Li L. Mathematical modelling for the pathogenesis of Alzheimer's disease. PLoS ONE 2010;5:e15176.
21. Berridge MJ. Calcium hypothesis of Alzheimer's disease. Eur J Physiol 2010;459:441-449.
22. Imbimbo BP, Solfrizzi V, Panza F. Are NSAIDs useful to treat Alzheimer's disease or mild cognitive impairment? Frontiers in aging neuroscience 2010:19.
23. Berridge M. Calcium signalling and Alzheimer's disease. Neurochem Res 2011;36:1149-1156.
24. Anastasio T. Data-driven modelling of Alzheimer disease pathogenesis. J Theor Biol 2011;290:60-72.
25. Camandola S, Mattson MP. Aberrant subcellular neuronal calcium regulation in aging and Alzheimer's disease. Biochim Biophys Acta 2011;965-973.
26. Ho M, Hoke D, Chua Y, et al. Effects of metal chelators on γ-secretase indicates that calcium and magnesium ions facilitate cleavage of Alzheimer amyloid precursor substrate. Int. J. Alzheimer's Dis 2011;950932.
27. Itkin A, Dupres V, Dufrêne Y, Bechinger B, Ruysschaert J-M, Raussens V. Calcium ions promote formation of amyloid b-peptide (1–40) oligomers causally implicated in neuronal toxicity of Alzheimer's disease. PLoS ONE 2011;6:18250.
28. Müller M, Cardenas C, Mei L, Cheung K-H, Foskett K. Constitutive cAMP response element binding protein (CREB) activation by Alzheimer's disease presenilin-driven inositol trisphosphate receptor (InsP3R) Ca2+ signaling. Proc Natl Acad Sci USA 2011;108:13293-13298.
29. Schmidt V, Baum K, Lao A, et al. Quantative modelling of amyloidogenic processing and its influence by SORLA in Alzheimer's disease. EMBO J 2011:1-14.
30. Ma T, Gong K, Yan Y, Song B, Zhang X, Gong Y. Mitochondrial modulation of store-operated Ca2+ entry in model cells of Alzheimer's disease. Biochim Biophys Res Commun 2012;426:196-202.

31. Woods N, Padmanabhan J. Neuronal calcium signaling and Alzheimer's disease. Adv Exp Med Biol 2012;740:1193-1217.
32. De Kimpe L, Bennis A, Zwart R, van Haastert E, Hoozemans J, Scheper W. Disturbed Ca2+ homoeostasis increases glutaminyl cyclase expression; connecting two early pathogenic events in Alzheimer's disease in vitro. PLoSONE 2012;7:44674.
33. Berridge M. Dysregulation of neural calcium signaling in Alzheimer disease, bipolar disorder and schizophrenia. Prion 2013;7:2-13.
34. Cabezas IL, Batista AH, Rol GP. The role of glial cells in Alzheimer disease: potential therapeutic implications. Neurologia (English Edition) 2014;29(5):305-309.
35. Chen JH, Ke KF, Lu JH, Qiu YH, Peng YP. Protection of TGF-β1 against neuroinflammation and neurodegeneration in Aβ1–42-induced Alzheimer's disease model rats. PloS one 2015;10(2):e0116549.
36. Von Bernhardi R, Cornejo F, Parada GE, Eugenin J. Role of TGFβ signaling in the pathogenesis of Alzheimer's disease. Frontiers in cellular neuroscience 2015;9:426.
37. Bertsch M, Franchi B, Marcello N, Tesi MC, Tosin A. Alzheimer's disease: a mathematical model for onset and progression. Math Med Biol 2016.
38. Hao W, Friedman A. Mathematical model on Alzheimer's disease. BMC systems biology 2016;10(1):1-18.
39. Forloni G, Balducci C. Alzheimer's disease, oligomers and inflammation. J Alzheimer s Disease 2018;62(3):1261-1276.
40. Kinney JW, Bemiller SM, Murtishaw AS, Leisgang AM, Salazar AM, Lamb BT. Inflammation as a central mechanism in Alzheimer's disease. Alzheimer's & Dementia: Translational Res, Clin Interventions 2018;4:575-590.
41. Zhu M, Wang X, Sun L, Schultzberg M, Hjorth E. Can inflammation be resolved in Alzheimer's disease? Therapeutic advances in neurological disorders 2018;11:1756286418791107.
42. Ozben T, Ozben S. Neuro-inflammation and anti-inflammatory treatment options for Alzheimer's disease. Clin biochem 2019;72:87-89.
43. Ali MM, Ghouri RG, Ans AH, Akbar A, Toheed A. Recommendations for anti-inflammatory treatments in Alzheimer's disease: a comprehensive review of the literature. Cureus 2019;11(5).
44. Ciuperca IS, Dumont M, Lakmeche A, et al. Alzheimer's disease and prion: An in vitro mathematical model. Discrete & Continuous Dynamical Systems-B 2019;24(10):5225.
45. Andrade-Restrepo M, Lemarre P, Pujo-Menjouet L, Tine LM, Ciuperca SI. Modeling the spatial propagation of Aβ oligomers in Alzheimer's Disease. ESAIM: Proceedings, Surveys 2020;67:30-45.
46. Rivers-Auty J, Mather AE, Peters R, Lawrence CB, Brough D. Anti-inflammatories in Alzheimer's disease-potential therapy or spurious correlate? Brain communications 2020;2(2):109.
47. Huang LK, Chao SP, Hu CJ. Clinical trials of new drugs for Alzheimer disease. Journal of biomedical science 2020;27(1):1-13.
48. Li H, Zhao H. Mathematical model of Alzheimer's disease with prion proteins interactions and treatment. Applied Mathematics and Computation 2022;433:127377.
49. Hu J, Zhang Q, Meyer-Baese A, Ye M. Finite-time stability and optimal control of a stochastic reaction diffusion model for Alzheimer's disease with impulse and time-varying delay. Applied Mathematical Modelling 2022;102:511-539.
50. Hao W, Lenhart S, Petrella JR. Optimal anti-amyloid-beta therapy for Alzheimer's disease via a personalized mathematical model. PLoS computational biology 2022;18(9):e1010481.
51. Al-Ghraiybah NF, Wang J, Alkhalifa AE, et al. Glial cell-mediated neuroinflammation in Alzheimer's disease. Int J molecular sci 2022;23(18):10572.
52. Pal S, Melnik R. Modelling of Anti-amyloid-Beta Therapy for Alzheimer's Disease. In: Int Work-Conf Bioinformatics, Biomed Eng 2023:431-442.
53. Van Dyck CH, Swanson CJ, Aisen P, et al. Lecanemab in early Alzheimer's disease. New Eng J Med 2023;388(1):9-21.
54. Ciuperca I, Pujo-Menjouet L, Matar-Tine L, Torres N, Volpert V. A qualitative analysis of an A β-monomer model with inflammation processes for Alzheimer's disease. Royal Society Open Sci 2024;11(5):231536.
55. Joëlle C, Genevieve D. The progression towards Alzheimer's disease described as a bistable switch arising from the positive loop between amyloids and Ca2+. J Theoretical Bio 2013;331:12-18.
56. Torres N, Molina E, Pujo-Menjouet L. An optimal control problem for anti-inflammatory treatments of Alzheimer's disease 2025.
57. Dhooge A, Govearts W, Kuznetsov AY. MATCONT: A Matlab package for numerical bifurcation analysis of ODEs. ACM transactions on Mathematical software 2003;29(2):141-164.
58. Dhooge A, Govaerts W, Kuznetsov YA, et al. CL_MATCONT A continuation toolbox in Matlab 2004.
59. Kuznetsov YA. Laminar-Turbulent Bifurcation Scenario in 3D Rayleigh-Benard Convection Problem. Elements of applied bifurcation theory. Springer, NY 1998.
60. Kuznetsov YA. Five lectures on numerical bifurcation analysis. Utrecht University, NL 2009.
61. Govaerts wJF. Numerical Methods for Bifurcations of Dynamical Equilibria. SIAM 2000.
62. Flores-Tlacuahuac A. Pilar Morales and Martin Riveral Toledo Multiobjective Nonlinear model predictive control of a class of chemical reactors. I & EC res 2012:5891-5899.
63. William EH, Laird CD, Watson JP, et al. Pyomo - Optimization Modeling in Python Second Edition 67.
64. Wächter A, Biegler L. On the implementation of an interior-point filter line-search algorithm for large-scale nonlinear programming. Math Program 2006;106:25-57.
65. Tawarmalani M, Sahinidis NV. A polyhedral branch-and-cut approach to global optimization. Mathematical Programming 2005;103(2):225-249.
66. Sridhar LN. Coupling Bifurcation Analysis and Multiobjective Nonlinear Model Predictive Control. Austin Chem Eng 2024a;10(3):1107.
67. Ranjan US. Optimal control for chemical engineers. Taylor and Francis 2013